Cancer Letters 294 (2010) 159–166

Contents lists available at ScienceDirect

Cancer Letters

journal homepage: www.elsevier.com/locate/canlet

Gold(III) porphyrin 1a inhibited nasopharyngeal carcinoma metastasis *in vivo* and inhibited cell migration and invasion *in vitro*

Ching Tung Lum [a,1], Xiong Liu [a,b,1], Raymond Wai-Yin Sun [a,1], Xiang-Ping Li [b], Ying Peng [c], Ming-Liang He [d], Hsiang Fu Kung [d,e], Chi-Ming Che [a,*], Marie C.M. Lin [a,e,*]

[a] *Department of Chemistry and Open Laboratory of Chemical Biology of the Institute of Molecular Technology for Drug Discovery and Synthesis, The University of Hong Kong, Pokfulam Road, Hong Kong, China*
[b] *Department of Otolaryngology, Nanfang Hospital, Nanfang Medical University, Guangzhou 510515, China*
[c] *Department of Neurology, The Second Affiliated Hospital, Sun Yat-Sen University, Guangzhou 510120, China*
[d] *Center for Emerging Infectious Diseases, The Chinese University of Hong Kong, Shatin, Hong Kong, China*
[e] *The State Key Laboratory in Oncology in Southern China, Cancer Center, Sun Yat-Sen University, Guangzhou, China*

ARTICLE INFO

Article history:
Received 16 October 2009
Received in revised form 31 December 2009
Accepted 26 January 2010

Keywords:
Gold(III) porphyrin 1a
Nasopharyngeal carcinoma (NPC)
Metastasis
Cell migration
Invasion

ABSTRACT

A physiologically stable gold compound, gold(III) *meso*-tetraphenylporphyrin (gold-1a), has been shown to be effective in inducing apoptosis and prolonging the survival of hepatocellular carcinoma (HCC)-bearing rats as well as inhibiting the tumor growth of mice bearing nasopharyngeal carcinoma (NPC), neuroblastoma and colon carcinoma. In this study, we showed that gold-1a prolonged the survival of NPC metastasis-bearing mice and inhibited intrahepatic and lung metastasis. Histologically, gold-1a markedly reduced tumor microvessel formation. Consistently, in *in vitro* studies, gold-1a inhibited migration and invasion of C666-1 human NPC cells. The data strongly support the use of gold(III) compounds to treat cancer metastasis.

1. Introduction

Nasopharyngeal carcinoma (NPC) is endemic to Southern China and Southeast Asia with particular prevalence in the Cantonese population [1]. In Hong Kong the incidence rate is around 20 per 100,000 persons per year [2]. Although NPC is highly radiosensitive and chemosensitive [1], the 5-year survival rate of patients suffering from this malignancy was only 19% following radiation therapy [2] due to distant metastasis in organs such as liver, lung and brain. Most of the mortalities are indeed associated with secondary metastasis of NPC in distant organs. Thus, novel strategies of NPC metastasis treatments are urgently needed.

The clinical achievement of cisplatin and its derivatives as anticancer agents has stimulated the progress of using metal-based compounds, including those of gold, for anticancer treatment. To this respect, extensive investigations on the anticancer activities of a variety class of gold compounds have been reported [3–8]. However, the development of gold(III) compounds as potential anticancer agents has been heavily hindered by their poor stability in solution, since gold in the +III oxidation state tends to be reduced *in vivo* to gold(I) or metallic gold in the reducing mammalian environment [9–11]. Recently we have synthesized a series of gold(III) *meso*-tetraarylporphyrins

* Corresponding authors. Addresses: Department of Chemistry and Open Laboratory of Chemical Biology of the Institute of Molecular Technology for Drug Discovery and Synthesis, 8/F, Kadoorie Biological Sciences Building, The University of Hong Kong, Pokfulam Road, Hong Kong. Fax: +852 28171006 (M.C.M. Lin), Department of Chemistry and Open Laboratory of Chemical Biology of the Institute of Molecular Technology for Drug Discovery and Synthesis, Room 505, Chong Yuet Ming Chemistry Building, The University of Hong Kong, Pokfulam Road, Hong Kong. Fax: +852 28571586 (C.M. Che).
E-mail addresses: cmche@hku.hk (C.-M. Che), mcllin@hkusua.hku.hk (M.C.M. Lin).
[1] These authors contributed equally to this work.

0304-3835/$ - see front matter © 2010 Elsevier Ireland Ltd. All rights reserved.
doi:10.1016/j.canlet.2010.01.033

which are stable against demetalation in physiological conditions [12]. Unlike other classes of gold(III) compounds, the rigid porphyrin ligand scaffolds in these compounds stabilize the gold(III) center. One of these compounds, gold-1a, was effective in killing multidrug-resistant KB-V1 human oral epidermoid carcinoma cells as well as cisplatin resistant CNE-1 human nasopharyngeal carcinoma cells [12]. Moreover, we reported elsewhere that, gold-1a induced apoptosis and prolonged the survival of hepatocellular carcinoma (HCC)-bearing rats [13] as well as inhibited the tumor growth of mice bearing nasopharyngeal carcinoma (NPC) [14], neuroblastoma [15] and colon carcinoma [16]. Microarray studies showed that gold-1a was capable of altering the transcription of genes related to apoptosis, p53 stabilization, cellular proliferation, angiogenesis, invasion, as well as metabolism [13].

In the present study, we employed an established NPC metastatic athymic mouse model to delineate the potential anti-NPC metastasis activities of gold-1a. As tumor cell migration and invasion plays pivotal roles in tumor metastasis, we then investigated whether gold-1a inhibited cell migration and invasion using a human NPC cell line C666-1. We also studied the expression profile of monoglyceride lipase (MGLL) which indirectly increases invasion [17,18] in response to gold-1a in C666-1 cells.

2. Materials and methods

2.1. Cell lines, growth media, growth conditions and drugs

Epstein-Barr virus (EBV)-positive human NPC cell line, C666-1 [19], was kindly provided by Dr. Dolly P. Huang from the Chinese University of Hong Kong. RPMI 1640 medium, fetal bovine serum (FBS) and trypsin–EDTA were products of Invitrogen (Carlsbad, CA). The C666-1 cells were maintained as monolayer culture in RPMI 1640 medium supplemented with 10% FBS (complete medium) at 37 °C, 5% CO_2. Gold-1a was synthesized as reported previously [12]. The compound was reconstituted either in PET diluent [20] (60% polyethylene glycol 400, 30% ethanol, 10% Tween 80) and then diluted with PBS for *in vivo* studies or in dimethyl sulfoxide (DMSO) for *in vitro* studies.

2.2. Animal model of NPC metastasis and experimental conditions

An established NPC metastasis mouse model was used in this study [21]. Male athymic mice (BALB/c nu/nu, 5–7 weeks old, weighting 15–22 g) were purchased from Charles River Labs (Wilmington, MA). Mice were maintained under specific pathogen-free conditions. All animal experiments were conducted under the guidelines approved by the Committee on the Use of Live Animals in Teaching and Research of the University of Hong Kong. Primary tumors were established by injection of 2×10^5 C666-1 cells suspended in 100 μl PBS directly into the liver under anesthesia with 1% pentobarbital sodium (40 mg/kg). The mice were then randomly divided into the following two groups with eight mice per group: (1) gold-1a (1 mg/kg) and (2) control. Gold-1a dissolved in PET diluent and then diluted in PBS or PBS supplemented with equal amount of PET diluent was first administrated 4 days after tumor inoculation by intraperitoneal injection once per day for 3 days according to the body weight to the gold-1a and control groups respectively. The mice were then allowed to rest for 2 days, and the treatments were repeated once per day for three more days. Another eight mice in each group were killed 13 days after tumor inoculation for tissue collection. The volume of PET diluent injected was kept $\leqslant 1$ μl in all mice, and mice in both gold-1a and control groups received the same amount of PET diluent.

2.3. Pathological and histological analysis

Tumor volume and degree of tumor metastasis were evaluated immediately after having sacrificed the animals. Tumor volume (V) was calculated by the formula $V = ab^2 \times 0.52$, where a and b were the longest and the shortest diameters of the xenografted tumor. Rate of growth inhibition of xenografted tumor was calculated by the formula $[(V_{\text{control group}} - V_{\text{experimental group}})/V_{\text{control group}}] \times 100\%$, where $V_{\text{control group}}$ was the tumor volume of mice treated with vehicle control; $V_{\text{experimental group}}$ was the tumor volume of mice treated with gold-1a. Livers and lungs of the mice were excised and fixed in 4% paraformaldehyde for 16 h, followed by embedding in paraffin for histological studies. Paraffin-embedded tissues were sectioned into 5 μm slices for histological studies. Tissue sections were stained with haematoxylin and eosin (H & E) and viewed under an inverted microscope at 400× magnification. For the detection of apoptotic cells in the mouse hepatoma tissues, *in situ* Cell Death Detection Kit (Roche, Penzberg, Bavaria, Germany) was used, and the procedures were described previously [13]. At the end of the experiment, the tissue sections were monitored under an inverted microscope at 400× magnification. Five fields were randomly chosen and the number of apoptotic cells was counted. Intra-tumoral microvessel density (iMVD) was determined by immunohistochemical staining for CD31. Monoclonal antibody against CD31 was purchased from Santa Cruz Biotechnology (Santa Cruz, CA). After dewaxing and rehydration, tissue sections were treated with 0.3% hydrogen peroxide in methanol for 10 min, followed by antigen retrieval by heating in sodium citrate in a microwave oven. After blocking, the sections were incubated with a diluted anti-CD31 antibody solution for 1 h. After washing with PBS, they were further incubated with horse radish peroxidase-conjugated secondary antibody for 30 min and incubated with diaminobenzidine substrate (Roche). The sections were counterstained with haematoxylin, dehydrated and mounted. iMVD was determined as previously described [22]. Briefly, highly vascularized areas in the tissue sections were identified under an inverted microscope. The number of microvessels per five microscopic fields (400× magnification) was taken as the value of iMVD. Five fields were randomly chosen for each tissue section.

2.4. Cell viability assay

Methylthiazolyldiphenyl-tetrazolium bromide (MTT) was purchased from Sigma–Aldrich (St. Louis, MO). C666-

1 cells were seeded at a density of 3×10^4 cells per well in 100 μl of complete medium in a 96-well plate 24 h before gold-1a treatment. The cells were treated with gold-1a at different concentrations in 100 μl of complete medium for 48 h. The concentration of DMSO was identical in each well and it was <0.05%. At the end of the experiment, 10 μl of 5 mg/ml MTT solution was added to each well, and the cells were incubated at 37 °C for 4 h. Two hundred microliters of acidic isopropanol (0.04 M hydrochloric acid in isopropanol) was then added to each well to dissolve the formazan complexes. Finally, the absorbance of the converted dye was measured at a wavelength of 570 nm with background subtraction at 620 nm. Each condition was done in triplicate and the data were shown as mean ± standard error of the mean (SEM) from at least three independent experiments.

2.5. Cell migration assay

C666-1 cells were seeded at 5×10^5 per well in a 6-well plate in 2 ml complete medium. Twenty-four hours later, a wound was induced across the well using a pipette tip. The cells were then either untreated or treated with gold-1a at 1 or 2 μM for 18 h. The final concentration of DMSO was identical in all wells (0.02%). At 0 and 18 h after wound induction, the cells were observed under an inverted microscope at 40× magnification. The percentages of cell migration were calculated by the formula $(x - y)/x \times 100\%$, where x and y were the relative widths of the wounds at 0 and 18 h respectively. Each condition was done in duplicate and the data were shown as mean ± SEM from three independent experiments.

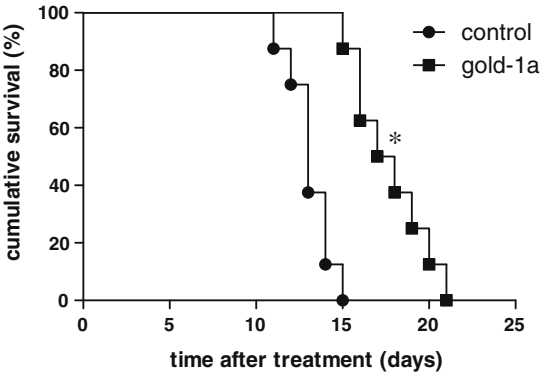

Fig. 1. Survival curves of NPC metastasis-bearing mice in control and gold-1a-treated groups. The median survivals of mice in control and gold-1a groups were 13 and 17.5 days respectively. $^*p = 0.0001$, compared to control group.

2.6. Cell invasion assay

BioCoat™ Matrigel™ Invasion Chamber is a product of BD Biosciences (San Jose, CA). Briefly, 0.75 ml of complete medium was added to the bottom of the well. At the same time, 5×10^4 cells resuspended in 0.5 ml complete medium with or without gold-1a (0.5 μM or 1 μM) were added to the insert of the well. The final concentration of DMSO was identical in all inserts (0.01%). The cells were then incubated at 37 °C, 5% CO_2 for 22 h. Non-invading cells in the interior of the insert were removed with cotton tips. Invaded cells were fixed with methanol for 2 min, followed by staining with 1% Toluidine Blue O (Sigma–Aldrich) and washing with water. The membrane was finally observed under an inverted microscope at 200× magnification. Ten fields were randomly chosen and the numbers of invaded cells were counted. The data were shown as mean ± SEM from three independent experiments.

2.7. Quantitative reverse transcriptase-polymerase chain reaction (qRT-PCR)

C666-1 cells were seeded at 2×10^6 per well in a 10-cm dish in 10 ml complete medium 24 h before treatment. Cells were untreated or treated with 2 μM gold-1a for 24 or 48 h. The concentration of DMSO was identical in all dishes (0.02%). Total RNA was then extracted using TRIZOL® Reagent (Invitrogen). Oligos were purchased from Sigma–Aldrich. The expression profiles of human glyceraldehyde-3-phosphate dehydrogenase (GAPDH) were used to normalize the mRNA levels of the target genes. Forward and reverse primers for human GAPDH and MGLL were 5′ TGGCGCTGAGTACGTCGTGG 3′ and 5′ TGGGGGCATCAGCAGAGGGG 3′, 5′ GCAGGTACTGGAAACCCACAGGC 3′ and 5′ TTCATAGCGGCCACTGTGCTCT 3′ respectively. One microgram of each total RNA sample was reverse transcribed to cDNA using SuperScript™ II Reverse Transcriptase (Invitrogen). The resulting first strand cDNA was diluted 10-fold and 1 μl of the diluted cDNA was then subjected to quantitative polymerase chain reaction (qPCR), using FastStart Universal SYBR Green Master (ROX) (Roche). The data were shown as mean ± SEM from three independent experiments.

2.8. Statistical analysis

Animal survival was analyzed by log-rank test using GraphPad Prism software (GraphPad Software Inc., San Diego, CA). Comparison of tumor volumes, numbers of metastasis nodules, iMVD values, cell numbers, percentages of cell migration and relative expression levels were

Table 1A
Effects of gold-1a in NPC-xenografted mice.

Group	Tumor volume (mm^3, $\bar{x} \pm$ SEM[a])	% of mice with liver metastasis (%)	% of mice with lung metastasis (%)	No. of lung metastasis nodules/animal ($\bar{x} \pm$ SEM[a])
Control	739.5 ± 43.4	100 (8 out of 8)	100 (8 out of 8)	3.58 ± 0.25
Gold-1a	358.4 ± 26.7[b]	50 (4 out of 8)	37.5 (3 out of 8)	1.34 ± 0.08[c]

[a] Mean ± standard error of the mean.
[b, c] $p < 0.0001$, compared to control.

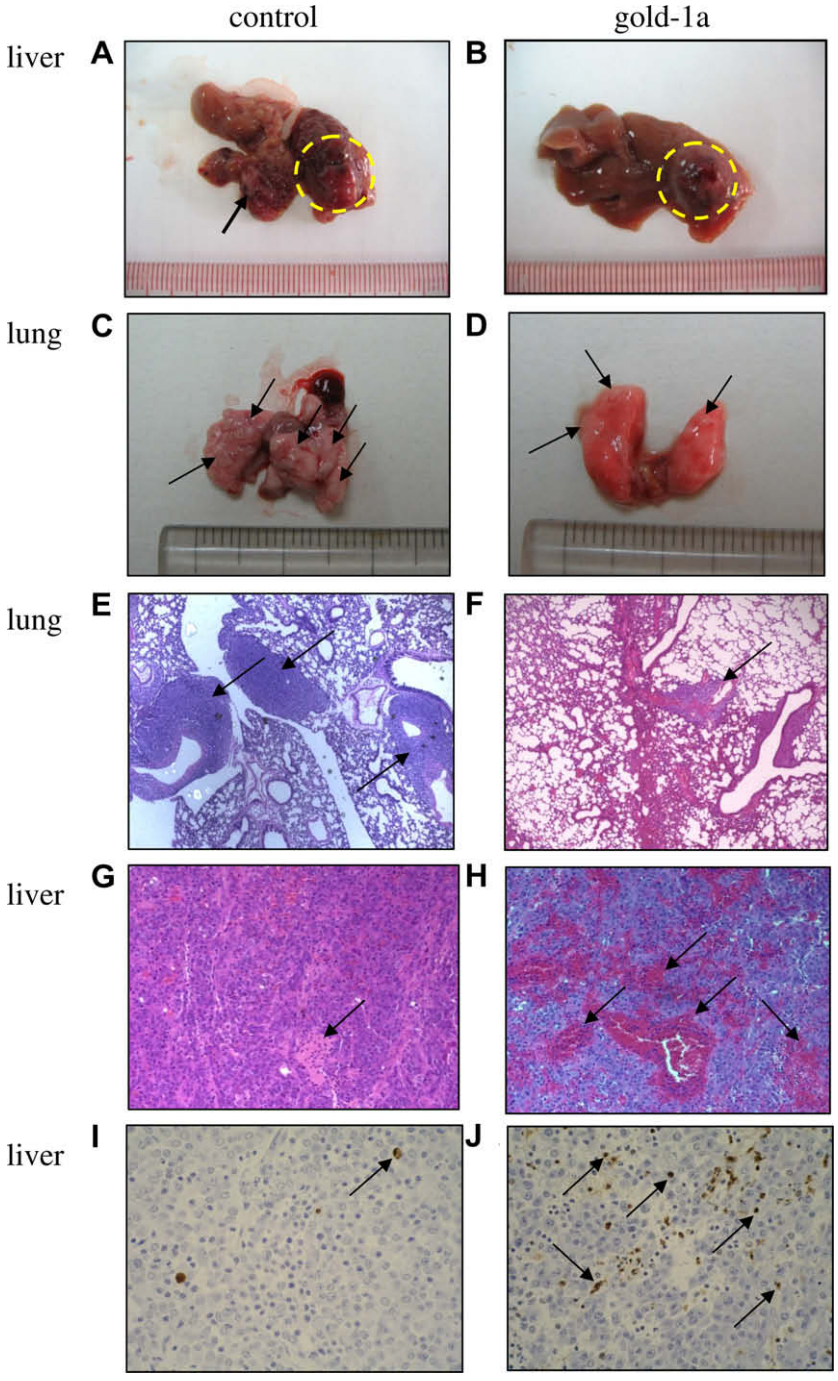

Fig. 2. (A,B) Morphologies of livers of mice in different experimental groups. (A) The numbers of metastasized tumors (arrow) were greater in the livers of mice in the control group. Arrow points to metastasized tumor and the inoculated tumor is circled. (B) The surfaces of the livers of mice in the gold-1a group were relatively smooth with little or no tumors, except for the locations where the tumors were inoculated (circled). (C,D) Morphologies of lungs of mice in different experimental groups. The number of metastasized tumor nodules in the lungs of the control group (C) was greater than those in the gold-1a group (D). Arrows point to the metastasized tumor nodules. (E,F) H & E staining of lung tissues of different treatment groups. Fewer tumor nodules were observed in the lungs of gold-1a-treated mice (F), compared to control mice (E). Arrows point to tumor nodules. (G,H) H & E staining of liver tissues of NPC metastasis-bearing mice. Obviously larger necrotic areas were found in the tumor tissues of gold-1a-treated mice (H), compared to control mice (G). Arrows point to necrotic areas. (I,J) TUNEL staining of primary liver tumor tissues of NPC metastasis-bearing mice. Greater numbers of positively-stained cells were found in the tissues in the gold-1a-treated group (J), compared to the control group (I). Arrows point to positively-stained apoptotic cells. Representative of eight mice in each group.

carried out using two-tailed Student's *t* test (MS Excel). $p < 0.05$ was considered statistically significant.

3. Results

3.1. Gold-1a prolonged the survival of NPC metastasis-bearing mice

To investigate whether gold-1a inhibit cancer metastasis, an established NPC metastasis mouse model was employed [21]. NPC metastasis-bearing mice were either treated with vehicle control or gold-1a, and there were eight mice in each group. The median survival times of mice in the control and gold-1a groups were 13 days and 17.5 days after treatment respectively (Fig. 1). Gold-1a significantly prolonged the survival of the NPC metastasis-bearing mice compared to vehicle control ($p = 0.0001$).

3.2. Gold-1a inhibited NPC primary tumor growth and prevented liver and lung metastasis

To investigate whether gold-1a inhibited primary tumor growth, eight NPC metastasis-bearing mice in each group were sacrificed 13 days after tumor inoculation and the tumor volumes were measured. To investigate whether gold-1a could prevent liver and lung metastasis, the morphologies of the livers and lungs were observed, and the numbers of lung metastasis nodules in the mice were counted after having sacrificed the animals. The average tumor volume of mice of the gold-1a group (358.4 ± 26.7 mm^3) was significantly smaller than that of the control group (739.5 ± 43.4 mm^3) (Table 1A), indicating that gold-1a was effective in inhibiting NPC primary tumor growth. Liver and lung morphologies from both groups were also examined. Livers of mice in the control group (Fig. 2A) displayed multiple metastasized tumors of different sizes on the surface (arrow). In contrast, the surfaces of the livers from gold-1a-treated mice (Fig. 2B) were relatively smooth with little sign of liver metastasis, except for the region containing the transplanted tumor (circled). Moreover, when we compared the percentages of intrahepatic metastasis between the two groups, we found that the percentage in the gold-1a group was 50% only, in contrast to 100% in the control group (Table 1A). Similar results were observed in the lungs. The average number of metastasis nodules in the lung of gold-1a group was significantly smaller (1.34 ± 0.08) than that in the control (3.58 ± 0.25) group (Fig. 2C and D, Table 1A). Consistent with the morphological observations in the lungs (Fig. 2C and D), H & E staining also showed larger and greater numbers of metastasis tumor areas in the lungs of control group (Fig. 2E) when compared to gold-1a (Fig. 2F) group.

Table 1B
Gold-1a downregulated iMVD in NPC-xenografted mice.

Group	iMVD[b] ($\bar{x} \pm$ SEM[a])	No. of apoptotic cells[c] ($\bar{x} \pm$ SEM[a])
Control	22.3 ± 1.1	5.5 ± 0.3
Gold-1a	10.5 ± 0.5[d]	56.3 ± 2.8[e]

[a] Mean ± standard error of the mean.
[b] Expressed as No. of microvessels per five microscopic fields.
[c] Expressed as No. of apoptotic cells per five microscopic fields.
[d, e] $p < 0.0001$, compared to control.

3.3. Gold-1a induced necrosis and apoptosis in the primary tumors of NPC metastasis mice

To investigate whether gold-1a induced necrosis and apoptosis in the tumor tissues, H & E staining and terminal deoxynucleotidyl transferase dUTP nick end labeling (TUNEL) were performed respectively in the tumor tissues from the eight mice in each group for examination of the histology of the tissues. Our results indicated that gold-1a treatment produced large areas of necrosis in the primary tumor tissues in the livers (Fig. 2H). In contrast, few necrotic areas were observed in the primary tumors of the control group (Fig. 2G). The numbers of apoptotic cells were also significantly greater in the primary liver tumor tissues of gold-1a-treated mice (Fig. 2J, Table 1B) compared to the mice in the control group (Fig. 2I, Table 1B), indicating that gold-1a was effective in inducing apoptosis in tumor tissues.

3.4. Gold-1a decreased intra-tumoral vascularization

To investigate whether gold-1a inhibited tumor vascularization, primary tumor tissues of the livers from eight mice in each group were immunostained with CD31 antibody for the detection of blood vessel endothelial cells. We demonstrated a significantly lower iMVD in the gold-1a group (10.5 ± 0.5), as compared to the control group (22.3 ± 1.1) (Fig. 3 and Table 1B), indicating that gold-1a was effective in decreasing intra-tumoral vascularization.

3.5. Gold-1a inhibited proliferation, migration and invasion of C666-1 human NPC cells

To determine the viabilities of C666-1 human NPC cells in response to gold-1a, MTT assay was performed on the cells. Our results indicated that gold-1a decreased the viabilities of C666-1 cells dose-dependently, with IC_{50} value of 0.75 ± 0.03 μM 48 h after treatment (Fig. 4A). To determine whether gold-1a inhibited migration of C666-1 cells *in vitro*, wound healing assay was performed, and we found from three independent experiments that gold-1a inhibited cell migration in a dose-dependent manner. At a dosage of 1 μM, gold-1a markedly inhibited migration of C666-1 cells, and the effect was more prominent when gold-1a was applied at 2 μM (Fig. 4B and C). We have also investigated the effect of gold-1a in invasion of C666–1 cells, and gold-1a was demonstrated from three independent experiments to inhibit cell invasion at both 0.5 and 1 μM (Fig. 4D and E).

3.6. Gold-1a downregulated the mRNA expression level of MGLL

To determine the mRNA expression level of MGLL in C666-1 cells in response to gold-1a treatment, qRT-PCR was performed on total RNA samples collected from DMSO- or gold-1a-treated C666-1 cells at 24

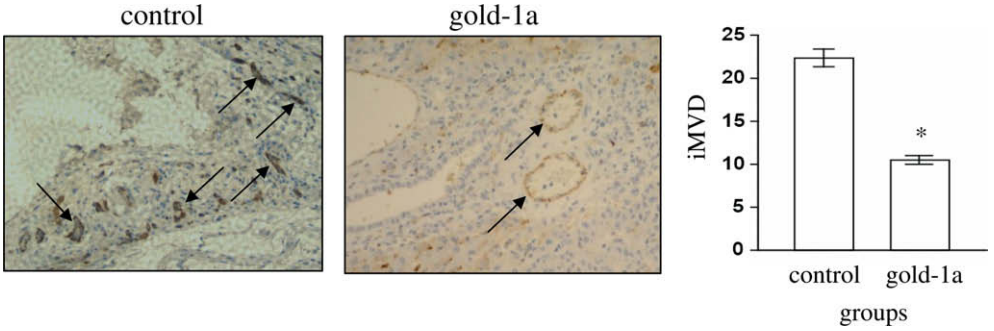

Fig. 3. Immunohistochemical detection of CD31 in the primary liver tumor tissues of mice in the control and the gold-1a-treated groups. Arrows point to CD31-positive microvessels. Representative of eight mice in each group. iMVD was significantly lower in the gold-1a group, compared to the control group. $^*p < 0.0001$, compared to the control group.

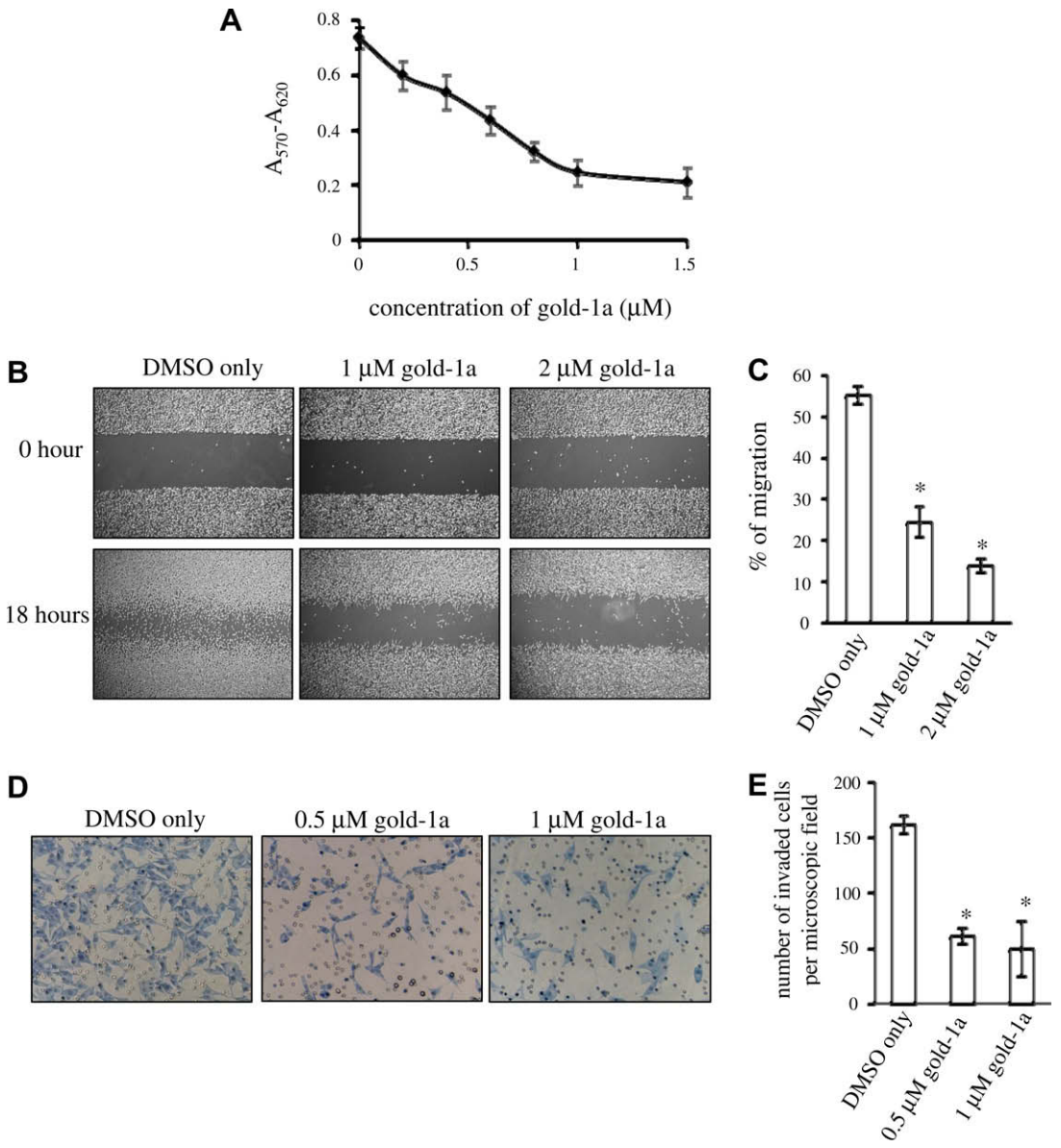

Fig. 4. (A) Viabilities of C666-1 cells in response to gold-1a treatment for 48 h. Gold-1a dose-dependently reduced the cell viability with IC_{50} value of 0.75 ± 0.03 μM. Data are shown as mean ± SEM from at least three independent experiments. (B) Wound healing assay showing that gold-1a dose-dependently inhibited cell migration. Photos were taken at 0 and 18 h after wound induction at 40× magnification. Representative of three independent experiments. (C) Graphical representation of the percentage of migration of C666-1 cells treated with different concentrations of gold-1a. Data were shown as mean ± SEM from three independent experiments. $^{*}p < 0.05$, compared to DMSO only. (D) Matrigel invasion assay showing that gold-1a inhibited cell invasion. Photos were taken at 200× magnification. Representative of three independent experiments. (E) Graphical representation of the numbers of invaded cells per microscopic fields when treated with different concentrations of gold-1a. Data were shown as mean ± SEM from three independent experiments. $^{*}p < 0.05$, compared to the DMSO only.

and 48 h. Gold-1a was demonstrated to downregulate the expression of MGLL at both time points, and the downregulation was statistically significant at 48 h (Fig. 5).

4. Discussion

Since the novel gold compound, gold-1a has been synthesized [12], it has been demonstrated to prolong the survival of HCC-bearing rats [13] as well as inhibit the tumor growth of mice bearing NPC [14], neuroblastoma [15] and colon carcinoma [16]. Mechanistically, induction of apoptosis played a major role [13,14,16]. In this study, we employed an established NPC metastasis mouse model [21] to study the efficacies of gold-1a in inhibiting tumor metastasis. In this model, highly metastatic EBV-positive C666-1 human NPC cells were inoculated into the livers of mice, and whether the tumors metastasized to other parts of the livers or to the lungs were observed. We demonstrated

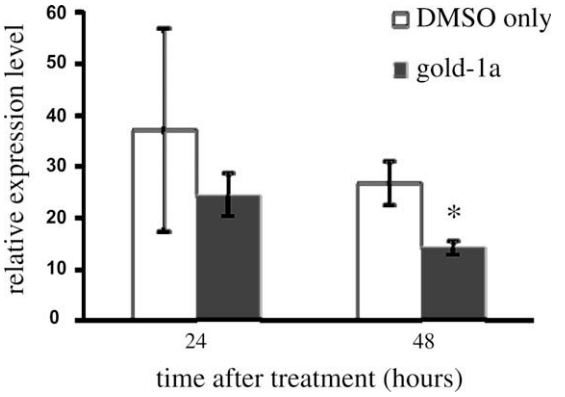

Fig. 5. Expression profile of MGLL in C666-1 cells in response to gold-1a treatment, as determined by qRT-PCR. Cells were treated either with DMSO only or with 2 μM of gold-1a for 24 or 48 h. The relative expression levels were compared to those of GAPDH. Data were shown as mean ± SEM from three independent experiments. $^{*}p < 0.05$, compared to DMSO only.

that gold-1a prolonged the survival of NPC metastasis-bearing mice and inhibited NPC metastasis. To our knowledge, the present study is the first *in vivo* preclinical study which demonstrates that gold(III) compound is capable of inhibiting tumor metastasis.

Cisplatin has been extensively used to treat various human solid carcinomas [23] and is currently the standard first-line chemotherapeutic treatment in NPC with a response rate of 80% [24,25]. However, the major hindrance to the use of cisplatin in treating NPC is the development of cisplatin resistance [26,27]. We have compared the efficacies of cisplatin in treating the NPC metastasis-bearing mice (data not shown) and found that when treated with 1.5 mg/kg of cisplatin, the percentages of mice with liver and lung metastasis were 75% and 62.5% respectively ($n = 8$), in comparison to 50% and 37.5% respectively ($n = 8$) when treated with 1 mg/kg of gold-1a. Moreover, the numbers of lung metastasis nodules in the mice treated with cisplatin or gold-1a were 2.86 ± 0.33 ($n = 8$) and 1.34 ± 0.08 ($n = 8$) respectively. These results provided clues that gold-1a might be superior to cisplatin in treating NPC metastasis.

Cell migration and invasion play pivotal roles in cancer metastasis [28,29]. In the present study, gold-1a was shown to inhibit metastasis *in vivo*. We therefore investigated whether gold-1a inhibited cell migration and invasion *in vitro* using the human NPC cell line C666-1. Consistent with the *in vivo* data, we found that gold-1a inhibited migration and invasion of C666-1 cells dose-dependently. Although the detailed molecular mechanism through which gold-1a inhibited migration and invasion remain elusive, we demonstrated that gold-1a downregulated MGLL in C666-1 cells. In a study which compared the gene expression profiles of medullary breast cancer and infiltrating ductal breast carcinoma with less favorable prognosis, MGLL was found to express only in the latter, and was expressed in 77% of these tumors [30]. The progression of ductal breast cancer shares features with cancer cell invasion [30], which supports the hypothesis that downregulation of MGLL may inhibit cell invasion. Furthermore, MGLL hydrolyzes 2-arachidonoylglycerol (2-AG) which inhibits invasion of cancer cells [17,18]. Downregulation of MGLL may therefore indirectly inhibit cancer cell invasion. 2-AG has been shown to inhibit migration of SW756 human papillomavirus 18-positive cervical carcinoma cells [31].

Apart from inhibition of cell migration and invasion, other mechanisms might also play important roles in gold-1a-mediated inhibition of metastasis. In addition to previously reported induction of apoptosis [13] and generation of reactive oxygen species [32], we have also demonstrated that gold-1a inhibited angiogenesis (data not shown). In the current study, despite the highly metastatic tumors, gold-1a displayed pronounced effects on inhibition of metastasis, suggesting that gold-1a might target multiple molecular pathways associated with growth, migration, invasion and angiogenesis. The current study provided preclinical evidence that gold-1a inhibit tumor metastasis, and therefore provided guidance for clinical trials in the future.

In summary, we demonstrated that gold-1a significantly inhibited NPC metastasis *in vivo* and inhibits cell migration and invasion *in vitro*. Moreover, the compound prolonged survival of the NPC metastasis-bearing mice. The present study demonstrated an unprecedented example of using gold(III) compound in inhibiting metastasis and invasion, and thus highlighted the possibility of using gold(III) compounds in treating cancer metastasis either alone or in combination with other agents.

Conflicts of interest

None declared.

Acknowledgements

This study was supported by grants from the AoE Scheme of UGC (AoE/P-10/01) and RGC (HKU7705/07 M to MCL) of the Hong Kong Special Administrative Region, China.

References

[1] Q. Tao, A.T. Chan, Nasopharyngeal carcinoma: molecular pathogenesis and therapeutic developments, Expert Rev. Mol. Med. 9 (2007) 1–24.
[2] B.B. Ma, E.P. Hui, A.T. Chan, Systemic approach to improving treatment outcome in nasopharyngeal carcinoma: current and future directions, Cancer Sci. 99 (2008) 1311–1318.
[3] M. Cagnoli, A. Alama, F. Barbieri, F. Novelli, C. Bruzzo, F. Sparatore, Synthesis and biological activity of gold and tin compounds in ovarian cancer cells, Anticancer Drugs 9 (1998) 603–610.
[4] M. Coronnello, E. Mini, B. Caciagli, M.A. Cinellu, A. Bindoli, C. Gabbiani, L. Messori, Mechanisms of cytotoxicity of selected organogold(III) compounds, J. Med. Chem. 48 (2005) 6761–6765.
[5] C. Gabbiani, A. Casini, L. Messori, A. Guerri, M.A. Cinellu, G. Minghetti, M. Corsini, C. Rosani, P. Zanello, M. Arca, Structural characterization, solution studies, and DFT calculations on a series of binuclear gold(III) oxo complexes: relationships to biological properties, Inorg. Chem. 47 (2008) 2368–2379.
[6] C.K. Li, R.W. Sun, S.C. Kui, N. Zhu, C.M. Che, Anticancer cyclometalated $[Au^{III}_m\ (C\hat{}N\hat{}C)_m\ L]^{n+}$ compounds: synthesis and cytotoxic properties, Chemistry 12 (2006) 5253–5266.
[7] G. Marcon, S. Carotti, M. Coronnello, L. Messori, E. Mini, P. Orioli, T. Mazzei, M.A. Cinellu, G. Minghetti, Gold(III) complexes with

bipyridyl ligands: solution chemistry, cytotoxicity, and DNA binding properties, J. Med. Chem. 45 (2002) 1672–1677.
[8] V. Milacic, D. Chen, L. Ronconi, K.R. Landis-Piwowar, D. Fregona, Q.P. Dou, A novel anticancer gold(III) dithiocarbamate compound inhibits the activity of a purified 20S proteasome and 26S proteasome in human breast cancer cell cultures and xenografts, Cancer Res. 66 (2006) 10478–10486.
[9] C.F. Shaw III, Gold-based therapeutic agents, Chem. Rev. 99 (1999) 2589–2600.
[10] R.W. Sun, D.L. Ma, E.L. Wong, C.M. Che, Some uses of transition metal complexes as anti-cancer and anti-HIV agents, Dalton Trans. 43 (2007) 4884–4892.
[11] E.R. Tiekink, Gold derivatives for the treatment of cancer, Crit. Rev. Oncol. Hematol. 42 (2002) 225–248.
[12] C.M. Che, R.W. Sun, W.Y. Yu, C.B. Ko, N. Zhu, H. Sun, Gold(III) porphyrins as a new class of anticancer drugs: cytotoxicity, DNA binding and induction of apoptosis in human cervix epitheloid cancer cells, Chem. Commun. 14 (2003) 1718–1719.
[13] C.T. Lum, Z.F. Yang, H.Y. Li, R.W. Sun, S.T. Fan, R.T. Poon, M.C. Lin, C.M. Che, H.F. Kung, Gold(III) compound is a novel chemo-cytotoxic agent for hepatocellular carcinoma (HCC), Int. J. Cancer 118 (2006) 1527–1538.
[14] Y.F. To, R.W. Sun, Y. Chen, V.S. Chan, W.Y. Yu, P.K. Tam, C.M. Che, C.L. Lin, Gold(III) porphyrin complex is more potent than cisplatin in inhibiting growth of nasopharyngeal carcinoma in vitro and in vivo, Int. J. Cancer 124 (2009) 1971–1979.
[15] W. Li, Y. Xie, R.W. Sun, Q. Liu, J. Young, W.Y. Yu, C.M. Che, P.K. Tam, Y. Ren, Inhibition of Akt sensitizes neuroblastoma cells to gold(III) porphyrin 1a, a novel antitumour drug induced apoptosis and growth inhibition, Br. J. Cancer 101 (2009) 342–349.
[16] S. Tu, R.W. Sun, M.C. Lin, J.T. Cui, B. Zou, Q. Gu, H.F. Kung, C.M. Che, B.C. Wong, Gold(III) porphyrin complexes induce apoptosis and cell cycle arrest and inhibit tumor growth in colon cancer, Cancer 115 (2009) 4456–4469.
[17] T.P. Dinh, D. Carpenter, F.M. Leslie, T.F. Freund, I. Katona, S.L. Sensi, S. Kathuria, D. Piomelli, Brain monoglyceride lipase participating in endocannabinoid inactivation, Proc. Natl. Acad. Sci. USA 99 (2002) 10819–10824.
[18] K. Nithipatikom, M.P. Endsley, M.A. Isbell, J.R. Falck, Y. Iwamoto, C.J. Hillard, W.B. Campbell, 2-Arachidonoylglycerol: a novel inhibitor of androgen-independent prostate cancer cell invasion, Cancer Res. 64 (2004) 8826–8830.
[19] S.T. Cheung, D.P. Huang, A.B. Hui, K.W. Lo, C.W. Ko, Y.S. Tsang, N. Wong, B.M. Whitney, J.C. Lee, Nasopharyngeal carcinoma cell line (C666-1) consistently harbouring Epstein-Barr virus, Int. J. Cancer 83 (1999) 121–126.
[20] S. Weitman, A.M. Langevin, R.L. Berkow, P.J. Thomas, C.A. Hurwitz, A.S. Kraft, R.L. Dubowy, D.L. Smith, M. Bernstein, A Phase I trial of bryostatin-1 in children with refractory solid tumors: a Pediatric Oncology Group study, Clin. Cancer Res. 5 (1999) 2344–2348.
[21] X.P. Li, C.Y. Li, X. Li, Y. Ding, L.L. Chan, P.H. Yang, G. Li, X. Liu, J.S. Lin, J. Wang, M. He, H.F. Kung, M.C. Lin, Y. Pen, Inhibition of human nasopharyngeal carcinoma growth and metastasis in mice by adenovirus-associated virus-mediated expression of human endostatin, Mol. Cancer Ther. 5 (2006) 1290–1298.
[22] N. Weidner, J. Folkman, F. Pozza, P. Bevilacqua, E.N. Allred, D.H. Moore, S. Meli, G. Gasparini, Tumor angiogenesis: a new significant and independent prognostic indicator in early-stage breast carcinoma, J. Natl. Cancer Inst. 84 (1992) 1875–1887.
[23] P. Kopf-Maier, Complexes of metals other than platinum as antitumour agents, Eur. J. Clin. Pharmacol. 47 (1994) 1–16.
[24] Q. Tao, A.T. Chan, Nasopharyngeal carcinoma: molecular pathogenesis and therapeutic developments, Expert Rev. Mol. Med. 9 (2007) 1–24.
[25] B.B. Ma, A.T. Chan, Systemic treatment strategies and therapeutic monitoring for advanced nasopharyngeal carcinoma, Expert Rev. Anticancer Ther. 6 (2006) 383–394.
[26] X. Wang X, J.R. Masters, Y.C. Wong, A.K. Lo, S.W. Tsao, Mechanism of differential sensitivity to cisplatin in nasopharyngeal, Anticancer Res. 21 (2001) 403–408.
[27] Y. Wang, Q.Y. He, S.W. Tsao, Y.H. Cheung, A. Wong, J.F. Chiu, Cytokeratin 8 silencing in human nasopharyngeal carcinoma cells leads to cisplatin sensitization, Cancer Lett. 265 (2008) 188–196.
[28] A. Raz, A. Ben-Ze'ev, Cell-contact and architecture of malignant cells and their relationship to metastasis, Cancer Metastasis Rev. 6 (1987) 3–21.
[29] J.C. Cheng, C.H. Chou, M.L. Kuo, C.Y. Hsieh, Radiation-enhanced hepatocellular carcinoma cell invasion with MMP-9 expression through PI3K/Akt/NF-kappaB signal transduction pathway, Oncogene 25 (2006) 7009–7018.
[30] M.F. Gjerstorff, V.M. Benoit, A.V. Laenkholm, O. Nielsen, L.E. Johansen, H.J. Ditzel, Identification of genes with altered expression in medullary breast cancer vs. ductal breast cancer and normal breast epithelial, Int. J. Oncol. 28 (2006) 1327–1335.
[31] M.I. Rudolph, Y. Boza, R. Yefi, S. Luza, E. Andrews, A. Penissi, P. Garrido, I.G. Rojas, The influence of mast cell mediators on migration of SW756 cervical carcinoma cells, J. Pharmacol. Sci. 106 (2008) 208–218.
[32] Y. Wang, Q.Y. He, R.W. Sun, C.M. Che, J.F. Chiu, GoldIII porphyrin 1a induced apoptosis by mitochondrial death pathways related to reactive oxygen species, Cancer Res. 65 (2005) 11553–11564.